JTTEE5 18:600–608
DOI: 10.1007/s11666-009-9391-5
1059-9630/$19.00 © ASM International

Antibacterial Property of Cold Sprayed Chitosan-Cu/Al Coating

Noppakun Sanpo, Siao Ming Ang, Philip Cheang, and K.A. Khor

(Submitted June 9, 2009; in revised form July 29, 2009)

The antibacterial behavior of CS-Cu (chitosan-copper complex) powder and their composite coatings were investigated against *Escherichia coli* (DH5α). CS-Cu powder and Al (aluminum) based CS-Cu composite powders were synthesized using in-house powder processing techniques. The results indicated that the antibacterial effect of all the powders increased with the proportion of CS-Cu powder. These composite powders were subsequently used as feedstock to generate antibacterial coatings via cold spray technology. The ratios of CS-Cu to Al in their composite powders were 25:75, 50:50, and 75:25 (wt.%). Microstructural characterization and phase analysis of feedstock powders and as-deposited coatings were carried out using FESEM/EDX and FTIR. Antibacterial composite CS-Cu/Al coatings were successfully deposited using cold spraying parameters of 6-8 bars at preheated helium gas, temperature between 140 and 150 °C. The coatings retained the antibacterial properties of the original feedstock powders.

Keywords aluminum composites, biomaterial, biomaterials of TS coatings, cold gas dynamic spraying, composite materials, nanostructured coatings, nanostructured materials

1. Introduction

Cold spraying is an emerging coating technology. A coating is formed by plastic deformation of sprayed particles in a solid state during impact in cold spraying. The temperature of spray particles prior to impact is much lower than their melting point and spray materials experience little microstructure change, oxidation, or decomposition (Ref 1).

Cold spraying is part of the large family of thermal spray processes and is now widely known as a materials deposition process for relatively small particles (ranging in size from approximately 1 to 50 μm in diameter). Most metals such as Cu-, Al-, Ni-, Ti-, and Ni-based alloys can be deposited by cold spray (Ref 1-4), and even cermets (Ref 5) and ceramics can be embedded into a substrate to form thin layered coatings. A potential advantage of this process over thermal spray is the ability to generate dense coatings while retaining their feedstock material chemistry and phase composition.

Aluminum is a particularly interesting cold spray candidate, for the following reasons: (i) Al may be used for a number of cosmetic, repair, and corrosion protection applications; (ii) it is a low density metal and thus may be accelerated to very high velocities by cold spray; and (iii) Al powders are available commercially in a variety of compositions (Ref 6). In previous works, Al-ZnO coatings were earlier deposited on glass at room temperature using cold spraying parameters (Ref 7). The results indicated that the antibacterial activity increased with increasing ZnO concentration in the composite powder feedstock and cold sprayed coating.

Medical implants are important to modern medicine and play an important role in the replacement and repair of human parts, ranging from organs to limbs (Ref 8). Metallic implants made from titanium and its alloys, stainless steel, cobalt-based alloys and so on, still dominate the implant market on account of their high mechanical properties and ease of machining (Ref 9). However, implant-related infections are considered to be common clinical complications that cause high rates of mortality and morbidity in orthopedic surgery, and the problem usually causes removal of the prosthesis and second operation, thus increasing health care costs.

It is well known that the success and long-term durability of these implants are impacted by the presence of bacteria in the vicinity of the implants. Bacterial infection after implant placement can cause significant complications, thereby increasing medical costs, morbidity, and patient dissatisfaction (Ref 10, 11).

These infections result from polymicrobial colonization on the surfaces of inert biomaterials and/or adjacent damaged tissue cells (Ref 11). Clinical practice has shown that systemic antibiotics are unable to provide effective treatment for these infections (Ref 10). It is now recognized

Noppakun Sanpo, School of Chemical and Biomedical Engineering, Nanyang Technological University, Singapore, Singapore; **Siao Ming Ang**, Industrial Research Institute Swinburne, Swinburne University of Technology, Melbourne, Australia; **Philip Cheang**, School of Science & Technology, SIM University, Singapore, Singapore; and **K.A. Khor**, School of Mechanical and Aerospace Engineering, Nanyang Technological University, Singapore, Singapore. Contact e-mails: Noppakuns@hotmail.com, AANG@groupwise.swin.edu.au, Philipcheanghn@unisim.edu.sg, Mkakhor@ntu.edu.sg.

that a high concentration of antibacterial agents at the bone-implant interface would be essential to prevent these bacterial infections (Ref 12).

The ideal medical implant should possess both antibacterial function and excellent cell biocompatibility. Therefore, means to mitigate bacterial infection and enhance biocompatibility on polymeric surfaces have aroused interest (Ref 13). It is recognized that implants with antibacterial performance would be essential to prevent these bacterial infections (Ref 9). Consequently, there is a need to find effective methods of surface modifications, capable of coating biomaterials with antibacterial agents such as silver and copper, to meet the specific demands of certain applications (Ref 12). Surface treatment techniques such as ultraviolet (UV) radiation, chemical and plasma grafting, ion implantation, and plasma immersion ion implantation and deposition (Ref 13-15) have been proposed. Experiments on plasma immersion ion implantation reveal that it is possible to embed inorganic copper and silver into the near surface region of organic polymers to improve the surface antibacterial properties (Ref 16). These two elements have less toxicity compared to other heavy metals. It is hoped that cold spray would be able to provide an alternative method of functionalizing a given material and impart antibacterial properties to it.

Chitosan, one of the most abundant natural polymers, is non-toxic, biodegradable, and biocompatible. Different from most other natural polymers, chitosan has high reactivity and processability for its specific molecular structure and polycationic nature (Ref 17). In recent years, chitosan and its derivatives received considerable attention due to their potential beneficial biological activities, such as biodegradability (Ref 18, 19), biocompatibility (Ref 20, 21), bioactivity (Ref 22, 23), and nontoxicity (Ref 24), that have been exploited for use in water treatment (Ref 25), papermaking (Ref 26), pharmaceutics (Ref 27), biotechnology (Ref 28), agriculture (Ref 29), and food processing (Ref 30). The antimicrobial activity of chitosan was observed against a wide variety of microorganisms including fungi, algae, and some bacteria (Ref 31). It is well known that metal ions, such as Ag^{+}, Cu^{2+}, Zn^{2+}, form an important group of antimicrobial agents, which have different active target from most bacteriostatic polymers. Chitosan is a powerful chelating agent, which is easy to form complexes with transition metals and heavy metals. Most researches of chitosan-metal complexes focused on their applications in the sequestration or removal of metal ions, dyeing, catalysis, water treatment, and many other industrial processes (Ref 32). Moreover, few researches pay attention to their biological activities. The mode of action is probably related to the binding of chitosan and copper, which is likely to leave some potential donor atoms free and these free donor atoms enhance the biological activity (Ref 33). However, the high toxicity of the copper-loaded complexes prevents their medicinal use as an antitumor agent. Zheng (Ref 34) was undertaken to synthesize copper complexes at different metal to chitosan ratios in attempt to reduce toxicity and to investigate its possible activity as an antitumor agent. The results showed that all of the copper complexes of chitosan inhibited the proliferation of the two tumor cell lines but not the normal human lung fibroblast cell line. Moreover, Qi (Ref 35) also studied the cytotoxic activity of copper-loaded chitosan and he found that copper-loaded chitosan showed high cytotoxic activity toward tumor cells, while low toxicity against normal human liver cells.

In a previous work (Ref 36), we also have found that CS-Cu complex had the best antibacterial property against Gram-positive bacteria.

The aim of this study was the deposition characteristics of cold sprayed CS-Cu/Al coating was examined using microstructural analysis of as-sprayed coatings comprising various ratios of CS-Cu/Al composite powders. The biofunctionality of CS-Cu/Al coating was also evaluated using bacteria assay to ascertain the killing rate against *Escherichia coli*.

2. Experimental Procedure

2.1 Materials

Chitosan, NaOH and $CuSO_4$ were purchased from Sigma-Aldrich, Germany. Aluminum powder of 99.8% purity (−45 μm) was purchased from CHT International Pte Ltd (Singapore). *E. coli* DH5α was provided by the Department of Biological Science of the Nanyang Technological University, Singapore.

2.2 Synthesis of CS-Cu Complexes

Chitosan sample was dissolved in diluted acetic acid to obtain a solution with concentration of 1%. By stirring, desired amount of metal ions (10 wt.% of copper salt) were added into the solution. The pH value was increased to 6.0 by dropping NaOH solution. After agitating for 3 h, the mixture was poured into excess of acetone. The precipitates collected by filtering were repeatedly washed with ethanol and finally dried under vacuum to constant weight. The dried CS-Cu flake was then crushed into powder using mortar and pestle before further use. The molecular structure of CS-Cu complex has reported that metal ion like a bridge connected one or more chains of chitosan through interacting with –OH and $–NH_2$ (Ref 33).

The samples were analyzed with JEOL JSM 6700-F field emission scanning electron microscope (FESEM) and energy dispersive x-ray spectrometer (EDX) for compositional analysis. Their antibacterial properties were tested against *E. coli* in Luria-Bertani broth and agar (both from Sigma-Aldrich). Moreover, the chemical bonding of CS-Cu complex also were determined by Fourier transform infrared spectroscopy (FTIR).

2.3 Cold Spray CS-Cu/Al Powders Preparation

CS-Cu powder has an irregular morphology as shown in Fig. 1. The commercially available aluminum powder

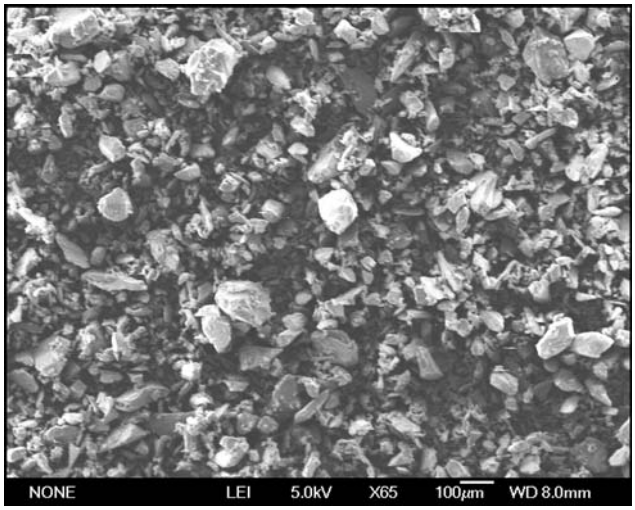

Fig. 1 SEM micrograph of CS-Cu powder

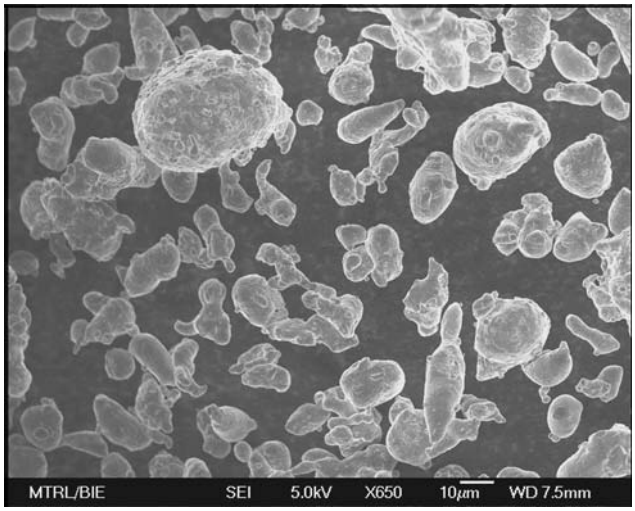

Fig. 2 SEM micrograph of Al powder

(−45 mesh) was used as an initial material. The aluminum powder has irregular morphology as shown in Fig. 2. Both powders that were used to generate the coatings were sieved to less than 45 μm before blending in a ball-mill for about 24 h. The CS-Cu and Al powders were mixed in a ratios of 25:75, 50:50, and 75:25 (wt.%).

2.4 Cold Spray Parameters CS-Cu/Al Powders

The cold spray system was obtained from the Russian Academy of Science, Siberia, and co-developed with ST Kinetics (Singapore) Engineering Company. An ABB Robot (IRB2400) was used in conjunction with the cold spray system. Glass slide will be cleaned with acetone and dried with pure air before using as coating substrate. Helium was used as the accelerating and carrier gas operating at pressures of 6 to 8 bars in the prechamber. The gas was preheated to a temperature of 140 to 150 °C. The standoff distance from the gun exit was 14 mm. The traverse speed of the gun relative to the substrate was 60 mm/s. The microstructure of the CS-Cu/Al coating was analyzed using a field emission scanning electron microscope (JEOL JSM-6700F).

2.5 LB Agar Plate and LB Broth Preparation

LB agar plate was prepared by dissolving LB agar powder in deionized water. The mixture was stirred and heated until the agar was completely dissolved. The solution was then autoclaved for 15 min at 121 °C to obtain a yellow solution. The agar solution was poured onto Petri dishes until fully covered. These agar plates were left uncovered inside a BioSafety cabinet for drying. Afterwards, the Petri dishes were then covered, stacked together, and sealed in plastic packaging. They were further placed inside a 37 °C incubator for 24 h to ensure that no bacteria contamination occurred during agar preparation. These agar plates were then stored in a 4 °C refrigerator.

LB broth was prepared by mixing LB broth powder with deionized water. The broth was stirred and dispensed into 10 mL test tubes. The solution was autoclaved for 15 min at 121 °C to obtain a yellow solution. The broth solution was stored in a 4 °C refrigerator.

2.6 Tests of Antibacterial Activity

The antimicrobial experiment was modified from Standard Test Method for Determining the Activity of Incorporated Antimicrobial Agent(s) in Polymeric or Hydrophobic Materials (ASTM E 2180), which is commonly used in School of Biological Science (SBS), Nanyang Technological University Singapore, to estimate the antimicrobial abilities of antimicrobial samples.

2.6.1 Bacterial Qualitative Test. The qualitative test of CS-Cu powder was prepared by compressing CS-Cu into pellet form (diameter about 2 cm). CS-Cu pellet was put on the top of LB agar surface which was covered with *E. coli*. The agar plates were placed upside down in a 37 °C incubator for 24 h before further analysis.

To perform qualitative analysis of the antibacterial properties of the CS-Cu/Al coating, LB agar solution was poured onto Petri dishes after the cold sprayed sample was placed perpendicular to the base of the Petri dish. Only half the sample was covered by the LB agar. *E. coli* was introduced onto the LB agar surface by using a micropipette to spread the bacteria over the agar surface. The agar plates were placed upside down in a 37 °C incubator for 24 h before further analysis.

2.6.2 Bacterial Quantitative Test. The *E. coli* stock was stored inside micro-centrifuge tubes at −80 °C. When required, the tubes were taken out and thawed at room temperature. A sterile wire loop was used to plate the bacteria by streaking lightly on the surface of agar coated petri dishes. Figure 3 shows the procedure of the first, second, and third streaking strokes on a single agar plate.

The agar plates were placed upside down in a 37 °C incubator for 24 h. Using a sterile wire loop, a single

Fig. 3 Schematic diagram of streaking bacteria

colony was extracted and streaked on to another agar plate. The plates were further incubated upside-down at 37 °C for another 24 h. Using a sterile wire loop, an isolated colony was placed into a test tube containing 10 mL of broth, and vortexed for 60 s. With a micro-pipette, 1 mL of *E. coli* solution was taken out and put into (a) pure broth 9 mL as a control; (b) broth 9 mL + sample 1; (c) broth 9 mL + sample 2; (d) broth 9 mL + sample 3, etc. This was followed by a number of serial dilutions, six times (up to 1:1,000,000).

In total, 100 μL of solution was plated onto agar dishes using a spreader. Where necessary, more than one plate was replicated for each concentration. The plates were again incubated at 37 °C (upside down) for 24 h. Choose and count the number of colonies in plates containing 30 to 300 colonies per plate. One colony represents a colony-forming unit (CFU).

Determine the geometric mean of the number of *E. coli* from the triplicate incubation period control and incubation period treated samples by the following equation:

$$\text{Geometric mean} = \frac{\log_{10} X1 \pm \log_{10} X2 \pm \log_{10} X3}{3}$$

where X is the number of organisms recovered from the incubation period control (glass without coating) or incubation period treated samples (glass with coating).

Percent *E. coli* reduction—Use the following equation to calculate the percent reduction:

$$\%\ E.\,coli\ \text{reduction} = \frac{(a-b)\times 100}{a}$$

where a is the antilog of the geometric mean of the number of *E. coli* from the incubation period control samples, b is the antilog of the geometric mean of the number of *E. coli* from the incubation period treated samples.

3. Results and Discussion

3.1 Microstructure of CS-Cu Complex and Cold Sprayed Coatings

3.1.1 Microstructure of CS-Cu Complex. Figure 1 shows the irregular shape of CS-Cu powder which has the same size about 20-60 μm. EDX results confirm that copper formed the complex with chitosan as shown in Table 1. Moreover, Fig. 4 shows the FT-IR spectra of chitosan and CS-Cu complex. The wide peak at 3430 cm^{-1}

Table 1 EDX result of CS-Cu powder

SEM picture	ZAF method standardless quantitative analysis		
	Element	Mass%	at.%
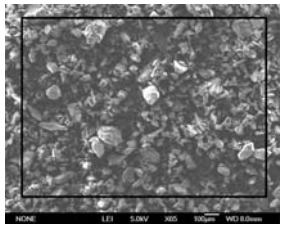	C	46.08	59.59
	O	37.48	36.39
	Cu	16.44	4.02
	Total		100

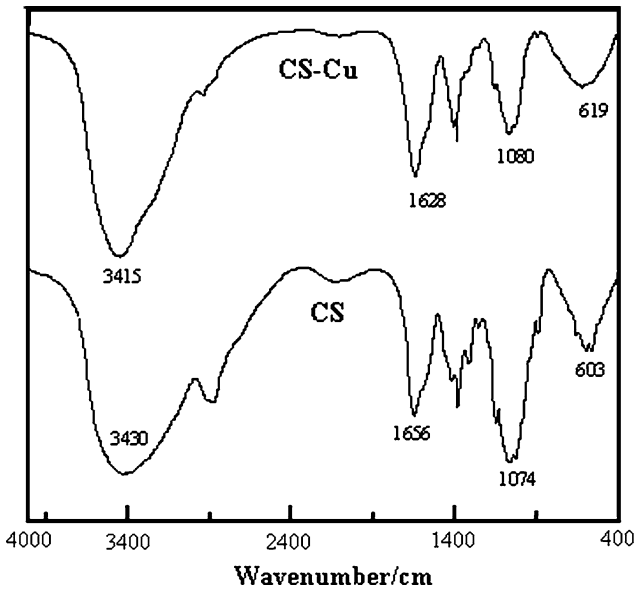

Fig. 4 FT-IR spectra of chitosan (CS) and chitosan-copper complexes (CS-Cu)

corresponding to the stretching vibration of $-NH_2$ group and –OH group shifted to lower frequency (3415 cm^{-1}) in the complexes, indicating $-NH_2$ or –OH groups take part in complexation. Absorption bands at 1656 cm^{-1} assigned to acetamide group and small peak at 1598 cm^{-1} assigned to "free" amine group appeared in CS spectra. Instead, an absorption band at 1628 cm^{-1} appeared, which was considered as the characteristic peak of the association of chitosan and metal in CS-Cu spectra. The band at 1080 cm^{-1}, 619 cm^{-1} assigned to ionic SO_4^{2-} was found in CS-Cu spectra, which indicated that SO_4^{2-} existed in the complex in the ionic form.

3.1.2 Microstructure of Cold Sprayed Coatings. Figure 5 shows the cold sprayed coating samples of (a) CS-Cu 25/Al 75, (b) CS-Cu 50/Al 50, and (c) CS-Cu 75/Al 25, respectively. The coating thicknesses of all samples were in the same range of about 50-60 μm.

SEM pictures of CS-Cu/Al coating are shown in Fig. 6(a) CS-Cu 25/Al 75, (b) CS-Cu 50/Al 50, and

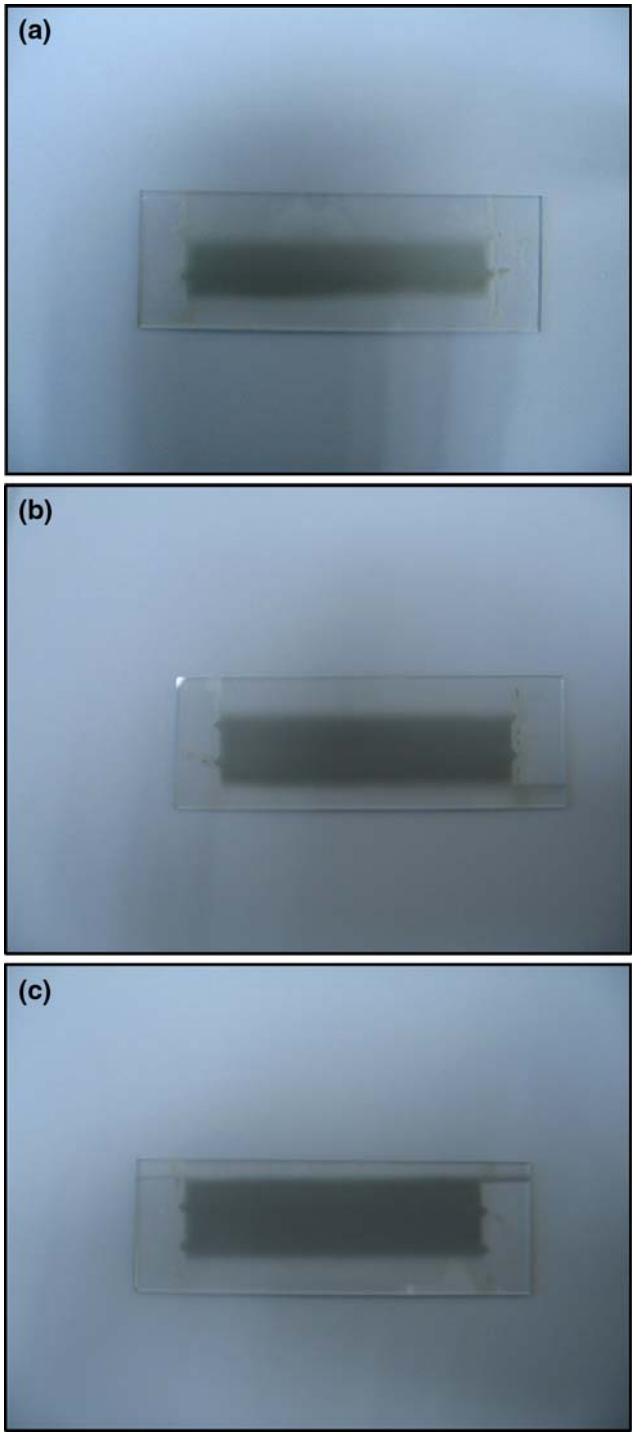

Fig. 5 Surface appearance of cold sprayed CS-Cu/Al coating on 7.5 × 2 cm glass slide with different compositions: (a) CS-Cu 25/Al 75, (b) CS-Cu 50/Al 50, and (c) CS-Cu 75/Al 25

(c) CS-Cu 75/Al 25, respectively. These images presented that the surface of cold sprayed coating consisted of CS-Cu powder embedded in a continuous Al matrix.

EDX results confirmed the presence of both CS-Cu/Al contents on the coating after cold spraying as shown in Table 2.

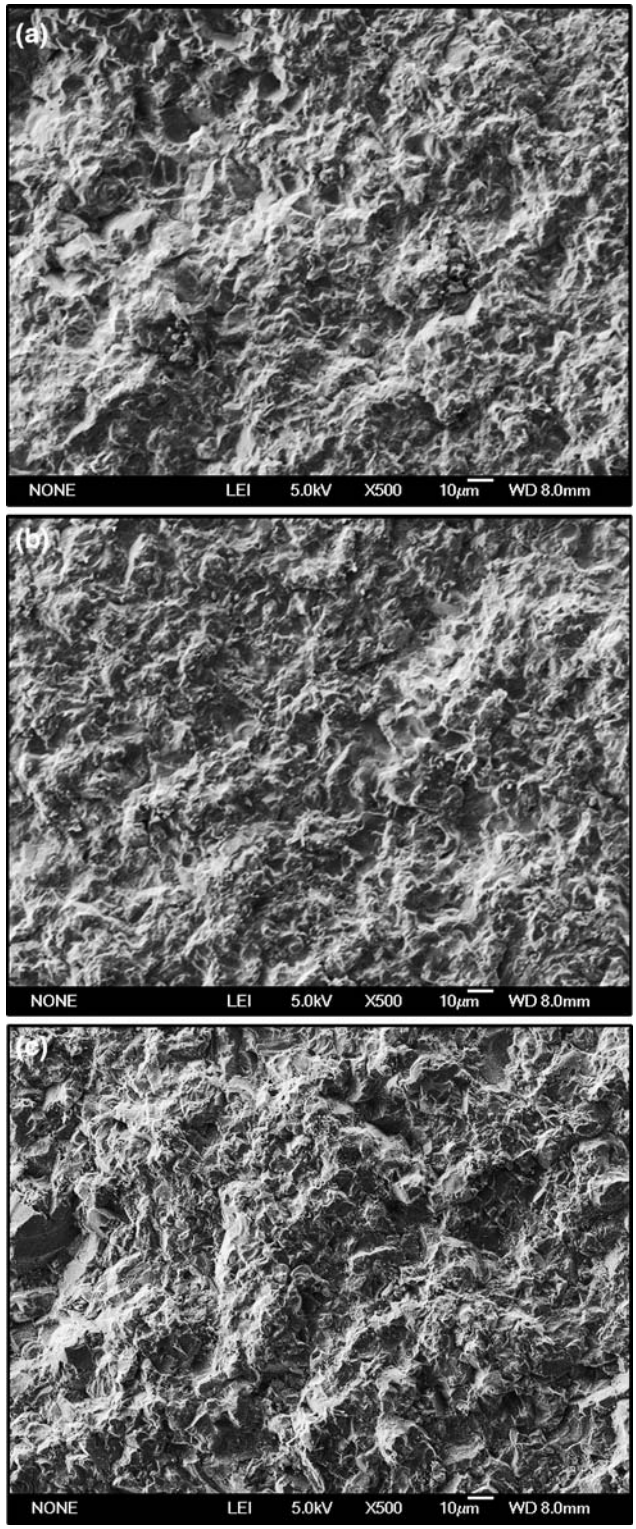

Fig. 6 SEM micrographs of CS-Cu/Al coating with different compositions: (a) CS-Cu 25/Al 75, (b) CS-Cu 50/Al 50, and (c) CS-Cu 75/Al 25

According to the EDX results of all CS-Cu/Al coatings, it can be stated that the composition of the Al of the cold sprayed coating was slightly higher than that of the

Table 2 EDX result of CS-Cu 75/Al 25 coating

SEM picture	ZAF method standardless quantitative analysis		
	Element	Mass%	at.%
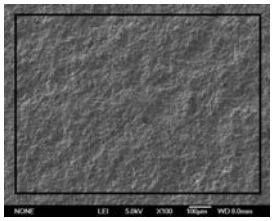	C	16.97	24.36
	O	51.37	56.26
	Al	5.89	3.76
	Si	24.23	14.87
	Cu	1.54	0.75
	Total		100

Table 3 The CS-Cu/Al contents (wt.%) in the powder feedstock and coatings

Powder composition	Powder feedstock		Coating	
	CS-Cu	Al	CS-Cu	Al
CS-Cu 25/Al 75	25	75	23	77
CS-Cu 50/Al 50	50	50	42	58
CS-Cu 75/Al 25	75	25	68	32

starting feedstock powder while the amount of CS-Cu was slightly lower than starting feedstock powder as shown in Table 3.

The formula used for calculation (wt.%) of CS-Cu and Al from EDX results is shown as follows:

$$\text{CS-Cu (wt.\%)} = \frac{\text{\% mass of [C + Cu]} \times 100}{\text{\% mass of [C + Cu + Al]}}$$

$$\text{Al (wt.\%)} = \frac{\text{\% mass of [Al]} \times 100}{\text{\% mass of [C + Cu + Al]}}$$

According to the backbone structure of CS-Cu and Al, carbon (C) and copper (Cu) were used for calculation CS-Cu (wt.%) while aluminum (Al) was used for calculation Al (wt.%).

Oxygen (O) and Silicon (Si) were ignored for calculation because it was found as the part of SiO_2 which was the main chemical structure of glass slide.

3.2 Antibacterial Results of CS-Cu Complex and Cold Sprayed Coating

3.2.1 Antibacterial Results of CS-Cu Complex. The antibacterial qualitative and quantitative results of CS-Cu complex are shown in Fig. 7 and 8, respectively. Obviously, the antibacterial activity of CS-Cu complex is much better than pure chitosan powder. Especially in qualitative result, the *E. coli* number of CS-Cu complex after 24 h is lower than pure chitosan result about 10^6 times. The calculation of percent reduction of *E. coli* is shown in Table 4. Pure chitosan powder does not show sufficient antibacterial result but CS-Cu powder presents about 70% of killing rate over *E. coli*.

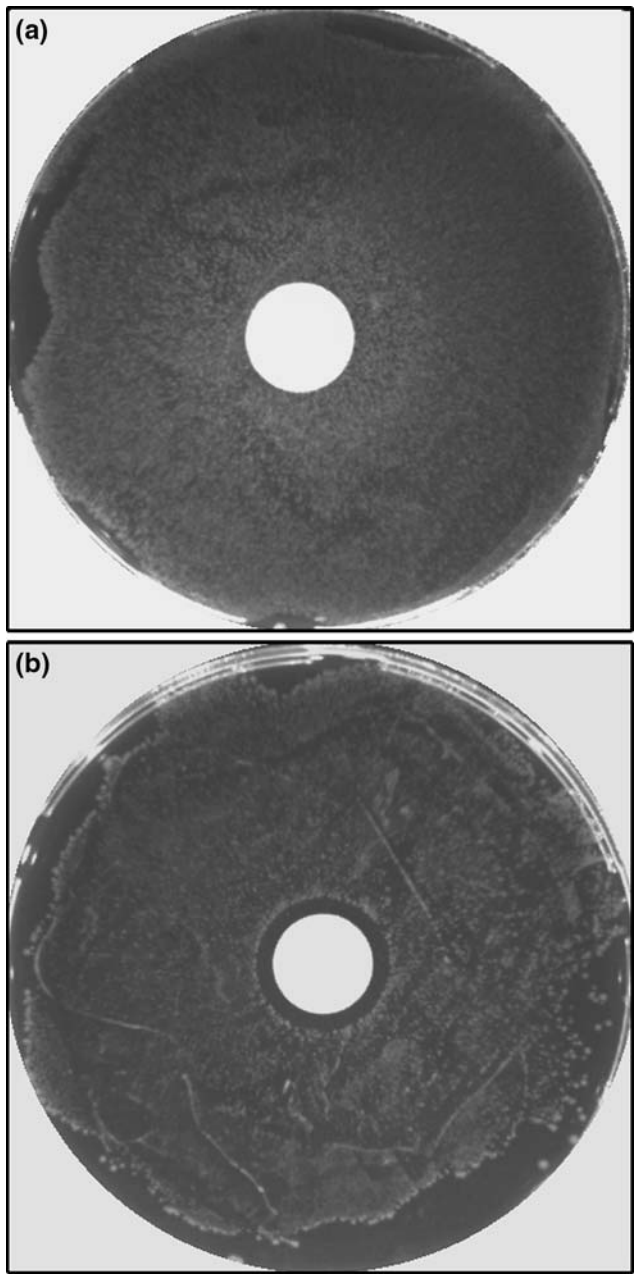

Fig. 7 Qualitative analysis on the antibacterial properties of CS-Cu powder. A clearance zone (absence of *E. coli* colonies) surrounding the sample pellet was observed on sample (b) CS-Cu powder compared with pure chitosan (a)

3.2.2 Antibacterial Results of Cold Sprayed Coating. Figure 9 shows that all cold sprayed samples have a very distinctive killing effect on *E. coli*. A lack of *E. coli* colonies growing in the region surrounding the CS-Cu coated samples was observed and appeared as clearance zone. The area of the clearance zone increased with

increasing CS-Cu powder concentration in the composite powder feedstock and cold sprayed coating, showing that the killing effect on *E. coli* increased with increasing amount of CS-Cu.

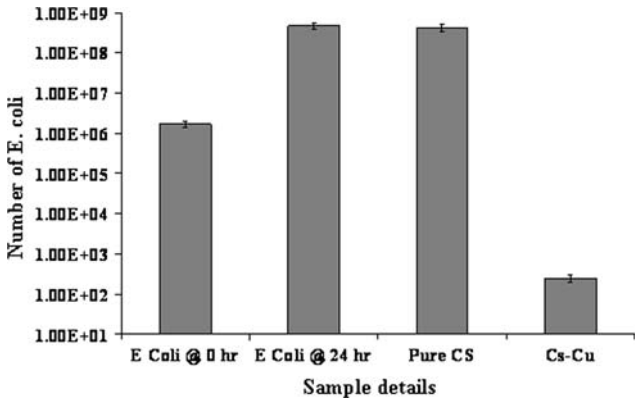

Fig. 8 Quantitative analysis on the antibacterial properties of CS-Cu powder

Figure 10 shows that all cold sprayed samples displayed an even more pronounced killing effect on *E. coli*. The killing rate increased with increasing CS-Cu powder concentration in the composite powder feedstock and cold sprayed coating. Table 5 presents the percent reduction of *E. coli* of CS-Cu 25/Al 75, CS-Cu 50/Al 50, and CS-Cu 75/Al 25 coatings which are 9.15, 14.96, and 22.08%, respectively. It can be clearly seen that the percent reduction of *E. coli* decreased with increasing CS-Cu composition on coating samples.

Table 4 The calculation of percent reduction of *E. coli* for CS-Cu powder

	Calculation	
Samples	**Geometric mean (X)**	**Percent reduction of *E. coli*, %**
Control sample (100% broth)	8.903	…
Pure chitosan	8.845	0.65
CS-Cu	2.699	70

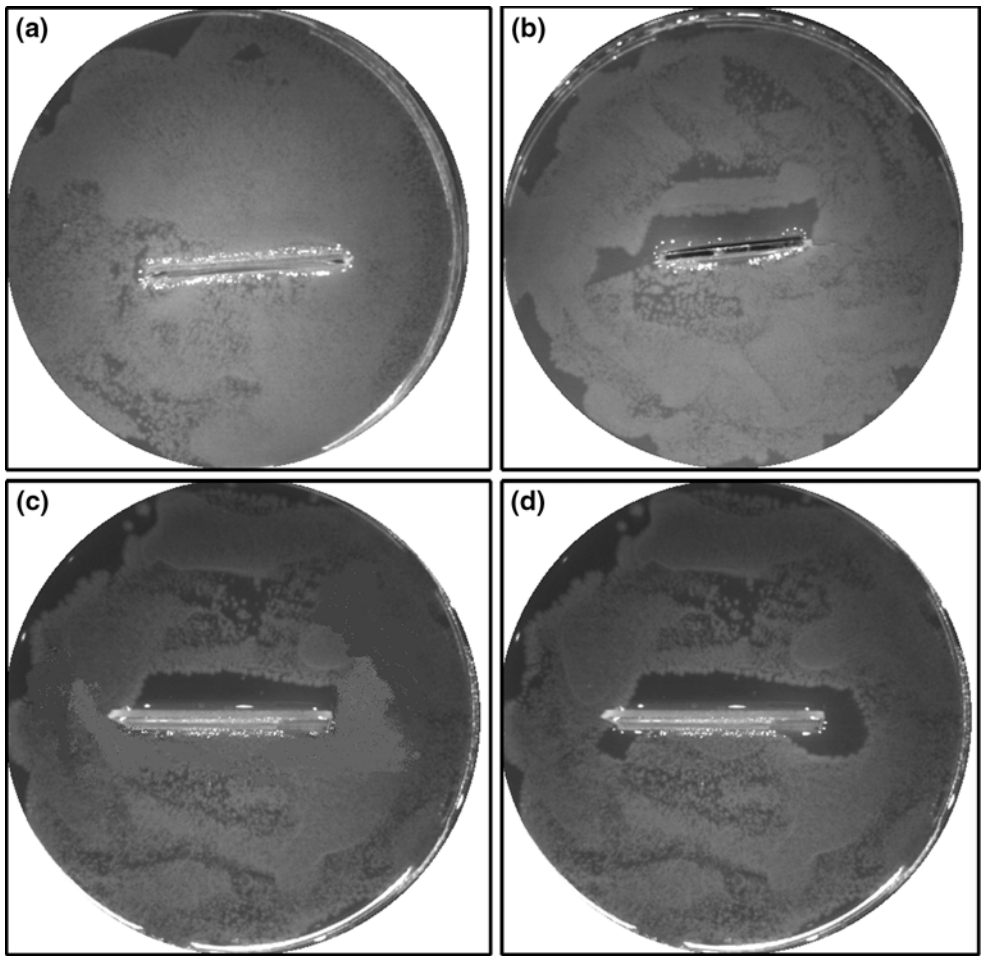

Fig. 9 Qualitative analysis on the antibacterial properties of CS-Cu/Al coatings. A clearance zone (absence of *E. coli* colonies) surrounding the coated samples was observed on samples (b), (c) and (d) in an increasing manner compared with glass without coating (a)

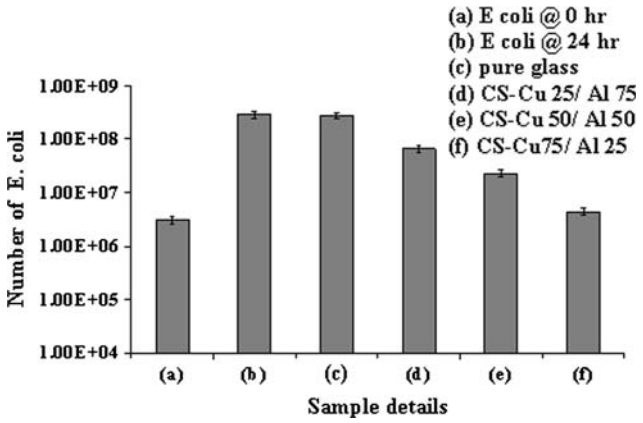

Fig. 10 Quantitative analysis on the antibacterial properties of CS-Cu/Al coatings

Table 5 The calculation of percent reduction of *E. coli* for CS-Cu/Al coatings

Samples	Calculation	
	Geometric mean (X)	Percent reduction of *E. coli*, %
Control sample (glass without coating)	8.699	…
CS-Cu 25/Al 75	7.903	9.15
CS-Cu 50/Al 50	7.398	14.96
CS-Cu 75/Al 25	6.778	22.08

4. Conclusions

CS-Cu/Al coatings were successfully deposited on glass at room temperature using cold spraying parameters of 6-8 bars at preheated helium gas, temperature between 140 and 150 °C. EDX analysis verified composition of the Al of the cold sprayed coating was slightly higher than that of the starting feedstock powder while the amount of CS-Cu on coating was slightly lower than starting feedstock powder. These as-sprayed coatings of varying CS-Cu/Al composition retained their inherent antibacterial property as clearly verified from bacteria assay. The results indicated that the antibacterial activity increased with increasing CS-Cu/Al powder concentration in the composite powder feedstock and cold sprayed coating. The experiment has shown that it is possible to cold spray a biopolymer complex (CS-Cu) when it is blended with ductile metal like aluminum.

Acknowledgments

We wish to acknowledge the funding support for this project (RG1/04) from Nanyang Technological University, and the joint research collaboration with ST Kinetics (Singapore).

References

1. R.C. McCune, W.T. Donlon, E.L. Cartwright, A.N. Papyrin, E.F. Rybicki, and J.R. Shadley, *Thermal Spray: Practical Solutions for Engineering Problems*, ASM International, Materials Park, OH, 1996, p 397-403
2. R.B. Bhagat, M.F. Amateau, A.N. Papyrin, J.C. Conway, Jr., B. Stutzman, Jr., and B. Jones, *Thermal Spray: A United Forum for Scientific and Technological Advances*, ASM International, Materials Park, OH, 1997, p 361-367
3. J. Karthikeyan, C.M. Kay, J. Lindeman, and R.S. Lima, *Thermal Spray: Surface Engineering via Applied Research*, ASM International, Materials Park, OH, 2000, p 255-262
4. T. Stoltenhoff, H. Kreye, H.J. Richter, and H. Assadi, *Thermal Spray 2001: New Surfaces for a New Millennium*, ASM International, Materials Park, OH, 2001, p 409-416
5. J. Karthikeyan, C.M. Kay, J. Lindeman, and R.S. Lima, *Thermal Spray: New Surfaces for a New Millennium*, ASM International, Materials Park, OH, 2001, p 383-387
6. W.B. Choi, L. Li, V. Luzin, R. Neiser, T. Gnaupel-Herold, H.J. Prask, S. Sampath, and A. Gouldstone, Integrated Characterization of Cold Sprayed Aluminum Coatings, *Acta Mater.*, 2007, **55**, p 857-866
7. N. Sanpo, T. Saraswati, T.M. Lu, and P. Cheang, Anti-Bacterial Property of Cold Sprayed ZnO-Al Coating, *BMEI*, 2008, **1**, p 488-491
8. W. Zhang, Y. Luo, H. Wang, S. Pu, and P.K. Chu, Biocompatibility of Silver and Copper Plasma Doped Polyethylene, *Surf. Coat. Technol.*, 2009, **203**, p 2550-2553
9. Y.Z. Wan, G.Y. Xiong, H. Liang, S. Raman, F. He, and Y. Huang, Modification of Medical Metals by Ion Implantation of Copper, *Appl. Surf. Sci.*, 2007, **253**, p 9426-9429
10. J. Mahan, D. Seligson, S.L. Henry, P. Hynes, and J. Dobbins, Factors in Pin Tract Infections, *Orthopedics*, 1991, **14**, p 305-308
11. A.G. Gristina, Biomaterial-Centered Infection: Microbial Adhesion Versus Tissue Integration, *Science*, 1987, **237**, p 1588-1595
12. Y.Z. Wan, S. Raman, F. He, and Y. Huang, Surface Modification of Medical Metals by Ion Implantation of Silver and Copper, *Vacuum*, 2007, **81**, p 1114-1118
13. B.D. Kalyon and U. Olgun, Antibacterial Efficacy of Triclosan-Incorporated Polymers, *Am. J. Infect. Control*, 2001, **29**, p 124-125
14. W. Chen, Y. Liu, H.S. Courtney, M. Bettenga, C.M. Agrawal, J.D. Bumgardner, and J.L. Ong, In Vitro Anti-Bacterial and Biological Properties of Magnetron Co-Sputtered Silver-Containing Hydroxyapatite Coating, *Biomaterials*, 2006, **27**, p 5512-5517
15. Y. Yuan, F. Ai, X. Zang, W. Zhuang, J. Shen, and S. Lin, Polyurethane Vascular Catheter Surface Grafted with Zwitterionic Sulfobetaine Monomer Activated by Ozone, *Colloids Surf. B*, **35**, 2004, p 1-5
16. W. Zhang, Y.-H. Zhang, J.-H. Ji, J. Zhao, Q. Yan, and P.K. Chu, Antimicrobial Properties of Copper Plasma-Modified Polyethylene, *Polymer*, 2006, **47**, p 7441-7445
17. C.J. Brine, P.A. Sandford, J.P. Zikakis, Antimicrobial Activity of Some Derivatives, *Advanced Chitin and Chitosan*, Elsevier, New York, 1992, p 543-548
18. H. Yamamoto and M. Amaike, Biodegradation of Cross-Linked Chitosan Gels by a Microorganism, *Macromolecules,* 1997, **30**, p 3936-3937
19. K. Tomihata and Y. Ikada, In Vitro and In Vivo Degradation of Films of Chitin and Its Deacetylated Derivatives, *Biomaterials*, 1997, **18**, p 567-575
20. S.C. Richardson, H.V. Kolbe, and R. Duncan, Potential of Low Molecular Mass Chitosan as a DNA Delivery System: Biocompatibility, Body Distribution and Ability to Complex and Protect DNA, *Int. J. Pharm.*, 1999, **178**, p 231-243
21. M.V. Risbud and R.R. Bhonde, Polyacrylamide-Chitosan Hydrogel: In Vitro Biocompatibility and Sustained Antibiotic Release Studies, *Drug Deliv.*, 2000, **7**, p 69-75
22. S. Dumitriu, M.I. Popa, A. Cringu, and A. Stratone, Bioactive Polymers 61. Synthesis and Characterization of Some Retard Antibiotics, *Colloid Polym. Sci.*, 1989, **267**, p 595-599

23. S. Matsuhashi and T. Kume, Enhancement of Antimicrobial Activity of Chitosan by Irradiation, *J. Sci. Food Agric.*, 1997, **73**, p 237-241
24. T. Chandy and C.P. Sharma, Chitosan Beads and Granules for Oral Sustained Delivery of Nifedipine: In Vitro Studies, *Biomaterials*, 1992, **13**, p 949-952
25. C. Huang, S. Chen, and J.R. Pan, Optimal Condition for Modification of Chitosan: A Biopolymer for Coagulation of Colloidal Particles, *Water Res.*, 2000, **34**, p 1057-1062
26. R.A.A. Muzzarelli, Chitin and Its Derivatives: New Trends of Applied Research, *Carbohydr. Polym.*, 1983, **3**, p 53-75
27. R. Bodmeier, H. Chen, and O. Paeratakul, A Novel Approach to the Oral Delivery of Micro- or Nanoparticles, *Pharm. Res.*, 1989, **6**, p 413-417
28. I. Tsigos, A. Martinou, D. Kafetzopoulos, and V. Bouriotis, Chitin Deacetylases: New, Versatile Tools in Biotechnology, *Trends Biotechnol.*, 2000, **18**, p 305-312
29. M. Bittelli, M. Flury, G.S. Campbell, and E.J. Nichols, Reduction of Transpiration Through Foliar Application of Chitosan, *Agric. For. Meteorol.*, 2001, **107**, p 167-175
30. W. Suntornsuk, P. Pochanavanich, and L. Suntornsuk, Fungal Chitosan Production on Food Processing By-products, *Process Biochem.*, 2002, **37**, p 727-729
31. I.R. Entsar, E.T.B. Moham, V.S. Christian, S. Gay, and S. Walter, Chitosan as Antimicrobial Agent: Applications and Mode of Action, *Biomacromolecules*, 2003, **4**, p 1457-1465
32. O.A. Odunola, Spectroscopic and Magnetic Properties of Zn(II), Cd(II) and Hg(II) Carboxylates, *Synth. React. Inorg. Met.-Org. Chem.*, 1993, **23**, p 1241-1249
33. R.G. Cuero, Antimicrobial Action of Exogenous Chitosan, *EXS,* 1999, **87**, p 315-333
34. Y. Zheng, Y. Yi, Y. Qi, Y. Wang, W. Zhang, and M. Du, Preparation of Chitosan–Copper Complexes and Their Antitumor Activity, *Bioorg. Med. Chem. Lett.*, 2006, **16**, p 4127-4129
35. L. Qi, Z. Xu, X. Jiang, Y. Li, and M. Wang, Cytotoxic Activities of Chitosan Nanoparticles and Copper-Loaded Nanoparticles, *Bioorg. Med. Chem. Lett.*, 2005, **15**, p 1397-1399
36. X. Wang, Y. Du, L. Fan, H. Liu, and Y. Hu, Chitosan-Metal Complexes as Antimicrobial Agent: Synthesis, Characterization and Structure-Activity Study, *Polym. Bull.*, 2005, **55**, p 105-113